4-15-1980

Modal Selection In Pulsating Stars

Norman R. Simon
University of Nebraska - Lincoln, nsimon@unl.edu

Arthur N. Cox
University of California, anc@lanl.gov

Stephen W. Hodson
University of California

THE ASTROPHYSICAL JOURNAL, 237:550–557, 1980 April 15

MODAL SELECTION IN PULSATING STARS

NORMAN R. SIMON
Theoretical Division, Los Alamos Scientific Laboratory, University of California;
and Behlen Laboratory of Physics, University of Nebraska–Lincoln

AND

ARTHUR N. COX AND STEPHEN W. HODSON
Theoretical Division, Los Alamos Scientific Laboratory, University of California
Received 1979 July 20; accepted 1979 October 2

ABSTRACT

Initial-value and periodic nonlinear pulsation integrations are carried out for a series of double-mode Cepheid models ($P_1/P_0 \sim 0.7$) in the vicinity of the resonance $\omega_1 + \omega_0 = \omega_3$. None of the models tested shows persistent double-mode behavior. A new, semiquantitative description of modal selection, based upon the iterative theory of Simon, is introduced to analyze the nonlinear results. In the simplest version of this description, modal section categories emerge which are identical to those of Stellingwerf. Our hydrodynamic results also agree at least partially with Stellingwerf's in that we find a region in the red where the models approach (though never reach) simultaneous instability of both limit cycles. Analysis of resonant effects on modal selection in our calculations leads to the conclusion that models lying between the resonances $\omega_1 + \omega_0 = \omega_3$ and $P_2/P_0 = 0.5$ may yet be viable candidates for double-mode pulsation.

Subject headings: stars: Cepheids — stars: pulsations

I. INTRODUCTION

The theoretical study of finite-amplitude, instability-strip pulsations has been complex and difficult. While the list of factors (both physical and numerical) affecting the theoretical models is substantial, the large amount of computer time required for nonlinear calculations restricts extensive parameter variation. The resultant need to extract general principles from limited investigations has hindered progress. Among the many basic questions still unsolved in this area, perhaps the most important and least understood involves the phenomenon of modal selection.

It is by now well known that, over a considerable portion of the instability strip, models exist which are simultaneously unstable to infinitesimal perturbations in more than one normal mode—most importantly, in the fundamental (F) and the first overtone (1O). At the same time, observations of pulsating stars have clearly demonstrated that in most domains only one of the unstable modes can persist at finite amplitude. While no certain method has yet been found to discern the pulsation mode of any given star, theoretical studies have succeeded in dividing various instability-strip domains into regions determined by properties of modal selection (e.g., Christy 1966 and Stellingwerf 1975*a* for the RR Lyrae stars; Stobie 1969 and King *et al.* 1973 for the classical Cepheids). Generally, these studies have agreed upon at least three regimes of different finite-amplitude behavior: (1) a region, beginning at the 1O blue edge and continuing somewhat beyond the F blue edge, where only 1O will persist; (2) a middle-temperature region where either F or 1O may be selected, depending upon initial conditions; and (3) an F only domain, still further to the red.

For the RR Lyrae case, such classifications seem to be consistent with certain observed properties, notably the Oosterhoff dichotomy (Stellingwerf 1975*a*). Similarly, for the middle-period or "bump" Cepheids, it appears that the modal selection categories are at least not in conflict with the observed Hertzsprung sequence (interpreted as involving fundamental mode pulsators), although severe conflicts may exist with the theory of stellar evolution (e.g., Simon and Schmidt 1976).

In spite of the partial successes that have been obtained, the theory of modal selection remains in a rather unsatisfactory state. Modal transition boundaries delineated in some of the studies have been sharply criticized (e.g., Cox 1979), while the physics underlying the modal selection problem remains as obscure as ever. The latter shortcoming is strongly underlined by our failure so far to deal satisfactorily with the phenomenon of multimode pulsation, whether in the regime of the double-mode Cepheids, or near the main sequence where the δ Scuti and AI Velorum pulsators are found.

In recent years, the advent of nonlinear, periodic integration techniques (Baker and von Sengbusch 1969; Stellingwerf 1974) has held out the promise of a new approach to the problems of modal selection. Stellingwerf (1975*a*, *b*) tested the stability of single-mode limit cycles and proposed modal selection categories on the basis of whether or not perturbations

corresponding to one of the modes would grow around the limit cycle of the other. Thus, when F grows in 1O, but 1O fails to grow in F, the fundamental is selected at limiting amplitude, and vice versa. When both limit cycles are stable, the final state depends upon initial conditions. Further, Stellingwerf suggested that the case of instability of both limit cycles ought to correspond to double-mode pulsation.

While the above ideas have been tested by nonlinear initial-value integrations in a handful of cases, they remain open to question for a number of reasons. In the first place, different results have sometimes been obtained by different workers treating the same models (e.g., Stellingwerf 1975*b*; Cox, Hodson, and Davey 1976; Hodson and Cox 1976). Furthermore, since the periodic integration technique will not necessarily detect all limit cycles, and certainly cannot find aperiodic final states, some doubt must arise as to both the necessity and sufficiency of Stellingwerf's categories. For example, if F grows in 1O but not vice versa, what is to guarantee that both modes will not persist after many cycles? Or, if both limit cycles are stable for a given model, how can it be ruled out that for certain initial conditions an aperiodic final state might also be reached? Clearly, such questions must be answered before the claim can be justified that periodic integration techniques can predict limiting-amplitude modal behavior.

An alternate approach to the problem of nonlinear pulsations involves the iterative theory (Simon 1972) which provides a means for calculating higher-order corrections to the linear pulsation quantities. A recent extension of this theory (Simon 1980, hereafter S80) has allowed the simultaneous treatment of two modes complete to second order, including lowest order modal interactions.

In an early paper, Simon and Sastri (1972) demonstrated, for the adiabatic case, that the second-order iterative correction terms are strongly influenced by resonances in the linear normal mode frequency spectrum. Later, this result was extended to nonadiabatic single-mode pulsations in classical Cepheid models (Simon 1977) and to the double-mode case (S80). At the same time, Simon (1979*a*) has suggested that the narrow range of period ratio observed in both the double-mode Cepheids and the double-mode AI Velorum stars is attributable to the influence of the interaction resonances $\omega_1 + \omega_0 = \omega_3$ and $\omega_1 + \omega_0 = \omega_4$ in the former and latter cases, respectively.

In the present investigation we study the problem of modal selection in a series of double-mode Cepheid models with period ratios close to the observed value ($P_1/P_0 \sim 0.70$), and lying in the vicinity of the resonance $\omega_1 + \omega_0 = \omega_3$. The aim of this work is twofold: first, to test the resonance hypothesis of Simon (1979*a*) in a specific case; second, to attempt to shed further light on the general problem of modal selection. Our procedures and results will be described in § II, while §§ III and IV will be given over to interpretation and discussion, including a semiquantitative description of modal selection based upon the iterative theory.

II. HYDRODYNAMIC INTEGRATIONS

a) Models and Techniques

The hydrodynamic integrations were performed with the code DYNSTAR, operating in both its initial value (Hodson and Cox 1976) and periodic (Cox, Hodson, and Davey 1976) modes. The models chosen for integration came from the principle series of S80, viz., $M = 3.3\ M_\odot$, $L = 1500\ L_\odot$, $X = 0.70$, $Z = 0.02$. Although convection may well be important in some of the cooler models, we have omitted it to make the calculations more manageable.

We note that the S80 and DYNSTAR calculations do not correspond precisely, since the static and linear nonadiabatic (LNA) models employed to initialize DYNSTAR differed slightly (and unavoidably) from the S80 versions for the same parameters and physical assumptions. Table 1 shows how these differences affected the linear period ratios P_1/P_0, the linear amplitude growth rates ϵ_0 and ϵ_1 (measured in percent per period) and the normalized distance to the resonance center, d_3 (Simon 1979*a*) for two specific models. In particular, one sees that the resonance center, $d_3 \approx 0$, is moved coolward some 150 K by DYNSTAR as compared with its location in the models of S80. We shall refer again to this circumstance later.

During the initial-value phase of the hydrodynamic calculations, the changing modal content of the oscillations was monitored by fitting the photospheric velocity variations with a third-order nonlinear Fourier-interaction series in which the two basic periods, P_0 and P_1, were also free parameters (Simon 1979*b*). Each of these fits included about 500 to 1000 time points. For models initiated at small amplitude, these points would, at the outset, encompass as many as 100 fundamental periods; but later, as limiting amplitude was approached, the points would cover only 10 fundamental periods, or even fewer. Standard deviations for these fits were typically less than 2 km s^{-1}, as compared with limiting amplitudes of 40 or 50 km s^{-1}.

TABLE 1

LNA PERIOD RATIOS AND GROWTH RATES: DYNSTAR VERSUS S80

	$T_e = 5800$ K		$T_e = 5500$ K	
PARAMETER	DYNSTAR	S80	DYNSTAR	S80
P_0	5.37	5.40	6.53	6.57
P_1/P_0	0.714	0.713	0.706	0.703
ϵ_0[a]	2.42	3.58	3.44	5.78
ϵ_1[a]	4.20	7.10	4.21	7.73
d_3	−0.025	−0.012	0.0017	0.027

[a] Measured in percent per period.

The question of exactly which properties of a given fit should be used to determine modal content has been answered differently by different investigators (e.g., Faulkner 1977; Cox, Hodson, and King 1978; Hodson, Stellingwerf, and Cox 1979; Shobbrook and Faulkner 1979). In the present study, we have monitored the amplitudes of the two basic frequencies, ω_0 and ω_1 (these amplitudes are called $A_0{}^1$ and $A_1{}^0$, respectively, in the notation of Simon 1979*b*), ignoring the harmonics and interaction terms which also emerge from the third-order fits. This interpretation is in line with the iterative theory in which the lower and higher order terms scale in a fixed pattern (Simon 1972), so that the amount present of $A_0{}^1$ and $A_1{}^0$ also determines the harmonic and interaction amplitudes. Furthermore, it is the lowest-order quantities which are needed for the comparisons we shall make with growth rates from LNA theory. In any event, since our interests are served by merely knowing the crude growth or decay rate for each mode at a given time (as opposed to a precise breakdown of the modal content), the results we shall report will be little influenced by our specific choice of monitoring technique.

b) Initial Conditions

The initial-value hydrodynamic integrations were all started by imposing velocity eigenfunctions from the LNA treatment of the respective models. The pulsations were initiated at small amplitude, characterized by a maximum photospheric velocity of 1 km s^{-1}. The initial velocity distributions were of two kinds: (1) the "half and half," in which the F and 1O eigenfunctions were superposed, each scaled to a photospheric value of $\frac{1}{2}$ km s^{-1}; and (2) the "pure F," which consisted of the fundamental eigenfunction alone, scaled to 1 km s^{-1} at the photosphere. We note that in both cases the initial distributions will inevitably contain some degree of noise, thus including a small amount of power at the frequencies of all the normal modes.

c) Preliminary Calculations

To begin our investigation, models at 5800, 5550, and 5500 K were initiated at small amplitude in the "half and half" condition. In each of these cases the pattern observed was the same: (1) an initial growth of each of the modes at respective rates consistent with those given by LNA theory, followed by (2) an abrupt quenching of the fundamental as the first overtone leveled off near limiting amplitude. Thus despite the proximity of these models to the resonance $\omega_1 + \omega_0 = \omega_3$, persistent double-mode behavior was not discovered.

Continuing our calculations, we initiated the 5500 K model at small amplitude with the "pure F" distribution. In this case the final outcome was opposite to that described above in that, following the initial phase of linear growth, the fundamental was able to establish itself at full amplitude, while the first overtone was extinguished.

Figure 1 shows the time evolution of the F and 1O amplitudes for both the "half and half" and "pure F" initiations in the model at 5500 K. One is struck by the abrupt switch from growth to decay of the "unwanted" mode, particularly 1O in the "pure F" initiation. The two cases plotted in Figure 1 obviously indicate that initial value integrations for the model in question will lead to different final states depending upon initial conditions. In the terminology of Stellingwerf (1975*a*), this ought to correspond to the case in which both limit cycles are stable. To check this, we employed DYNSTAR in its periodic mode to determine limit cycles for both F and 1O. Each did indeed turn out to be stable.

Table 2 compares some initial growth rates determined from the hydrodynamic integrations (HYD) with those given by LNA calculations also produced by DYNSTAR. The HYD rates were read crudely from curves like those given in Figure 1. We note from Table 2 that the HYD values are less than their LNA counterparts by amounts ranging from 25 to 50%. The discrepancies are smaller at 5500 K where the zoning of the LNA version (50 zones) approximated the HYD zoning, than at 5800 K where the LNA model had 195 zones. When one takes into account differences between LNA and HYD numerics along with the approximate method of determining HYD growth rates, the agreement seems good enough to allow the assertion that the initial growth of the hydrodynamic amplitudes crudely agrees with that predicted by LNA

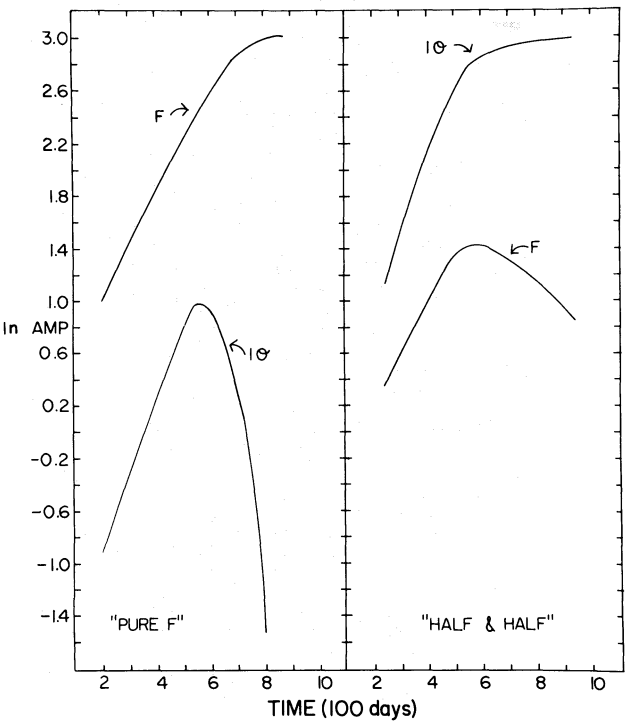

FIG. 1.—Time evolution of F and 1O amplitudes in initial-value integrations for the DYNSTAR model at 5500 K. *Left*, "pure F" initiation; *right*, "half and half" initiation.

TABLE 2

LINEAR AND NONLINEAR GROWTH RATES

MODE	INITIATION	GROWTH RATES[a] HYD	LNA
	$T_e = 5800$ K		
F	Half and half	1.44	2.42
1O	Half and half	2.59	4.20
	$T_e = 5500$ K		
F	Half and half	2.49	3.44
F	Pure F	2.72	3.44
1O	Half and half	2.86	4.21
1O	Pure F	2.68	4.21

[a] Measured in percent per period.

theory. One may further read from Table 2 the reassuring result that initial hydrodynamic growth rates for each mode were essentially independent of initial conditions in the model at 5500 K.

III. A THEORY OF MODAL SELECTION

We begin this section by considering the hydrodynamic integrations for the 5500 K model, displayed in Figure 1. These results seem to indicate that the mode which reaches the nonlinear regime first is the one which ultimately becomes established. Thus, an initial velocity distribution of equal parts F and 1O favors the latter due to its larger linear growth rate, while imposition of "pure F" (i.e., with a small, inevitably present, mixture of 1O and other modes) gives the fundamental enough of a head start to overcome the more rapid rise of the overtone. This description appears to be consistent with the results of King *et al.* (1973), who found that initially imposed fundamental velocity distributions would establish themselves at full amplitude unless the linear growth rate of 1O was relatively large, in which case the overtone was selected.

A useful perspective on these results may be obtained by considering the simpler case of the approach to limiting amplitude for a single mode. We may give a heuristic picture of the process as follows: The oscillation is driven from "beneath" by the linear instability and damped from "above" by the nonlinear corrections. Since the relative size of the nonlinear terms is a function of amplitude, the limiting amplitude is reached when nonlinear damping just balances linear driving.

Applying this picture to the case of bimodal pulsations, one finds that it suffices only for the established mode. The other, 'unwanted" mode abruptly loses its "linear support" and is thus extinguished. We shall try to further model this process using the iterative theory. We recall that, in this scheme, the pulsation is built up, order by order, beginning with the two basic frequencies ω_0 (fundamental) and ω_1 (first overtone). The relative importance of the various orders is determined by the amplitude of each mode which may be measured by a pair of scale factors—λ_0 for the fundamental, and λ_1 for the overtone. The terms of first order scale like λ_0 or λ_1, the second-order terms like quadratic products of these factors, the third-order terms like cubic products, etc. Table 3 shows the frequencies which emerge, and their scaling, up to third order.

TABLE 3

FREQUENCIES UP TO THIRD ORDER IN THE ITERATIVE THEORY

Order	Frequency	Scaling	Description
1	ω_0	λ_0	Linear
	ω_1	λ_1	Linear
2	$2\omega_0$, 0	λ_0^2	Harmonic
	$2\omega_1$, 0	λ_1^2	Harmonic
	$\omega_1 \pm \omega_0$	$\lambda_0\lambda_1$	Interactive
3	$3\omega_0$, ω_0	λ_0^3	Harmonic
	$3\omega_1$, ω_1	λ_1^3	Harmonic
	$2\omega_0 \pm \omega_1$, ω_1	$\lambda_0^2\lambda_1$	Interactive
	$2\omega_1 \pm \omega_0$, ω_0	$\lambda_1^2\lambda_0$	Interactive

One notes that the frequencies appearing in Table 3 are linear combinations of the two basic frequencies (ω_0 and ω_1) and are, in fact, the same as those which are obtained from Fourier fitting of observed light curves (Simon 1979*b* and references therein). For our purposes the important fact to notice from Table 3 is that in third order the original frequencies reappear, so that corrections are added to the amplitudes and phases of the linear eigenfunctions. Furthermore, it can be seen that these corrections are of two distinct sorts: (1) harmonic terms, which involve only the scale factor of the mode being corrected; and (2) interactive terms, which involve both scale factors.

Table 4 shows the scaling of the linear terms and corresponding third-order corrections, for each of the two basic frequencies. In the simplest possible interpretation, the third-order corrections damp the pulsation by distorting the linear eigenfunctions until they can no longer produce net driving. In this sense, the *harmonic* corrections are to be associated with the *single-mode* case, described heuristically above. The competition between linear driving and nonlinear harmonic damping is decided only by the scale factor of the mode in question, i.e., by its amplitude.

On the other hand, one sees from Table 4 that the ratio of *interactive* damping to linear driving depends not upon the amplitude of the mode considered, but rather upon that of the competing mode! Thus there

TABLE 4

SCALING OF LINEAR AMPLITUDES AND THIRD-ORDER CORRECTIONS IN THE ITERATIVE THEORY

FREQUENCY	FIRST ORDER	THIRD ORDER Harmonic	Interactive
ω_0	λ_0	λ_0^3	$\lambda_1^2\lambda_0$
ω_1	λ_1	λ_1^3	$\lambda_0^2\lambda_1$

must exist some value of λ_1 (say $\mathscr{L}_1$) beyond which the fundamental will be interactively damped, and some value of λ_0 (say $\mathscr{L}_0$) beyond which the overtone can no longer maintain itself. If we now define the single-mode limiting amplitudes for F and 1O as Λ_0 and Λ_1, respectively, four distinct categories emerge from the analysis:

a) $\Lambda_1 > \mathscr{L}_1$, $\Lambda_0 < \mathscr{L}_0$. In this case, F will be suppressed before 1O reaches its limiting amplitude, but not vice versa. Thus the final state must be 1O. This case is exactly equivalent to Stellingwerf's (1975*a*) category (expressed in terms of growth rates of one of the modes about the limit cycle of the other): 1O in F > 0, F in 1O < 0.

b) $\Lambda_1 < \mathscr{L}_1$, $\Lambda_0 > \mathscr{L}_0$. This is just the opposite of case (*a*), and is equivalent to Stellingwerf's 1O in F < 0, F in 1O > 0.

c) $\Lambda_1 > \mathscr{L}_1$, $\Lambda_0 > \mathscr{L}_0$. Here either mode is capable of suppressing the other, provided it can become large enough before being suppressed itself. Thus the mode which wins the race to finite amplitude will ultimately establish itself. Clearly, the 5500 K model discussed above falls into this category which is equivalent to Stellingwerf's 1O in F < 0, F in 1O < 0.

d) $\Lambda_1 < \mathscr{L}_1$, $\Lambda_0 < \mathscr{L}_0$. Here neither mode can suppress the other. According to Stellingwerf, this is the case of double-mode pulsation, characterized by 1O in F > 0, F in 1O > 0.

Consider now a hypothetical experiment in which one of the modes (say 1O) is held fixed at a given amplitude (λ_1) while the other mode (in this case F) is left free to seek a limit. Repetition of this experiment on a given model will produce a function $\Lambda_0(\lambda_1)$. In a similar way, reversing these roles determines a function $\Lambda_1(\lambda_0)$. We thus introduce the concept of the limiting amplitude of a given mode as a function of the (fixed) size of the other mode.

Figures 2*a*–2*d* show schematic representations of the functions $\Lambda_0(\lambda_1)$ and $\Lambda_1(\lambda_0)$. In each case, the former (*solid curve*) is plotted against the ordinate λ_1, and the latter (*dashed curve*) against the abscissa λ_0. To obtain the general form of the graphs given in Figure 2, the simplest possible assumptions have been made—namely, that both functions are strictly monotonic and that they cross at most once. The former assumption corresponds physically to the circumstance in which the interactive third-order corrections always alter the linear eigenfunctions in such a way as to reduce the driving, no matter what the size of λ_0 or λ_1.

It can be easily seen that Figures 2*a*, 2*b*, 2*c*, and 2*d* correspond, respectively, to the modal selection categories (a), (b), (c), and (*d*), given above. The single-mode limiting amplitudes $\Lambda_0(0)$ and $\Lambda_1(0)$, as well as the suppression amplitudes $\mathscr{L}_0$ and $\mathscr{L}_1$, have been entered schematically. Arrows on the diagrams crudely indicate the evolution direction of system points (λ_0, λ_1) in various regions of the amplitude-amplitude space. In Figure 2*c*, a double-mode pulsation point exists where the two curves intersect, but this point is unstable. On the contrary, the intersection in Figure 2*d* is a stable point of double-mode pulsation. As indicated by the arrows for this case, the system must eventually relax to a bimodal state.

Thus, provided that the functions $\Lambda_0(\lambda_1)$ and $\Lambda_1(\lambda_0)$

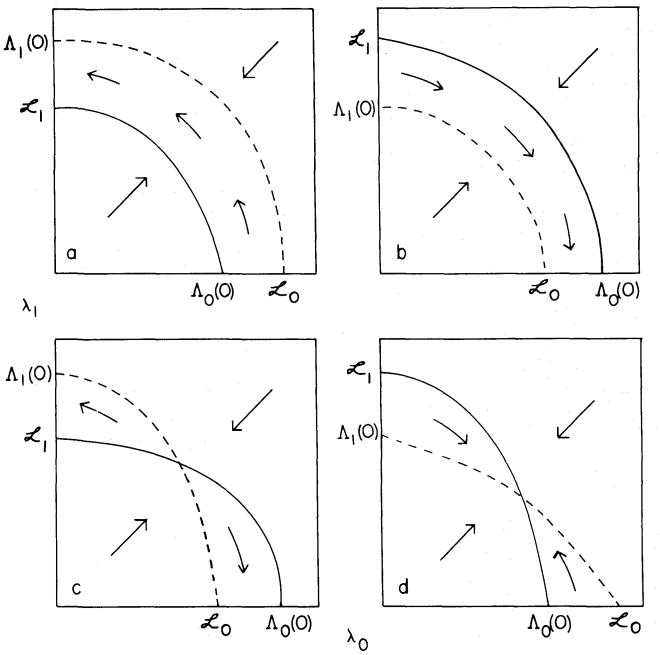

FIG. 2.—Schematic representations of the functions $\Lambda_0(\lambda_1)$ (*solid curves*) and $\Lambda_1(\lambda_0)$ (*dashed curves*) for the four categories (*a*–*d*) given in the text. In each case, the abscissa λ_0 measures the amount of F, and the ordinate λ_1 the amount of 1O. The single-mode limiting amplitudes, $\Lambda_0(0)$ and $\Lambda_1(0)$, and suppression amplitudes, $\mathscr{L}_0$ and $\mathscr{L}_1$, have been indicated. Arrows show how system points evolve in the amplitude-amplitude space.

are indeed monotonic and cross not more than once, the Stellingwerf categories will be absolute, and, in particular, the criterion for double-mode pulsation (i.e., instability of both limit cycles) will be both necessary and sufficient. On the other hand, there is no *a priori* reason to believe that the interactive terms will necessarily be damping at all amplitudes for all models. If we abandon this assumption, then the possibility exists of diagrams much more complex than those displayed in Figure 2. In particular, one may easily construct cases in which a system point in the amplitude-amplitude diagram executes cyclic evolution around an intersection of the functions $\Lambda_0(\lambda_1)$ and $\Lambda_1(\lambda_0)$. Such an evolution could explain the modal changes which seem to be occurring in TU Cas (Hodson, Stellingwerf, and Cox 1979; Niva 1979) and perhaps in U TrA (Shobbrook and Faulkner 1979). Of course, if this suggestion is correct, we must expect to see at some time in the future a reversal in the direction of modal evolution in these two stars.

The interpretations presented in this section may be made more concrete by a further examination of the initial-value integrations for the model at 5500 K. In Figure 3, the data from these integrations (already presented in Fig. 1) have been replotted in amplitude-amplitude space. The quantities $A_0{}^1$ and $A_1{}^0$ refer to the F and 1O amplitudes, respectively. One sees that approximate values for the crucial limits $\Lambda_0(0)$, $\mathscr{L}_0$, $\Lambda_1(0)$, and $\mathscr{L}_1$ may be read directly from this graph. These have been indicated. It is interesting to note along the ordinate of this plot the relatively small distance separating $\Lambda_1(0)$ and $\mathscr{L}_1$. Since it is the sign of the quantity $\Lambda_1(0) - \mathscr{L}_1$ which distinguishes category (*b*) from category (*c*), one might suspect that the 5500 K model does not lie too far from a modal transition line. To test this proposition, periodic integrations using DYNSTAR were performed on a model with $T_e = 5300$ K. The fundamental limit cycle was found to be stable; the overtone limit cycle, unstable. Thus the transition between (*b*) and (*c*) behavior was found to lie between 5500 and 5300 K.

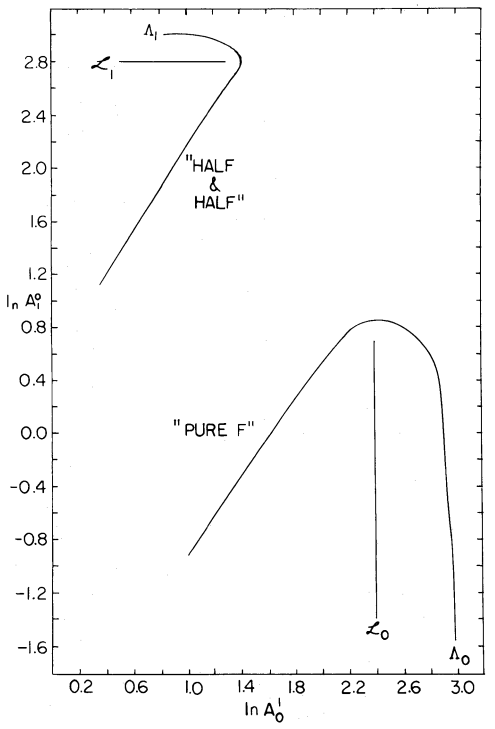

FIG. 3.—Amplitude-amplitude plot of the data for the 5500 K model treated in Fig. 1. *Abscissa*, F amplitude; *ordinate*, 1O amplitude. *Top curve*, "half and half" initiation; *bottom curve*, "pure F" initiation. Limiting amplitudes (Λ_0 and Λ_1) and suppression amplitudes ($\mathscr{L}_0$ and $\mathscr{L}_1$), as read from these curves, are indicated.

IV. DISCUSSION

Up to this point, we have studied the growth of pulsations in a handful of models, and offered an interpretation of the modal selection process based on the iterative theory. No evidence has been found for stable double-mode pulsation in any of the models tested despite their proximity to the resonances $\omega_1 + \omega_0 = \omega_3$ and $P_2/P_0 = 0.5$. Nevertheless, we shall argue in what follows that the prognosis for the resonance hypothesis is perhaps not so dim as these negative results might indicate.

Figure 4 shows fundamental and first overtone growth rates (in percent per period) plotted against effective temperature over a range of models. The two lower curves come from periodic integrations using

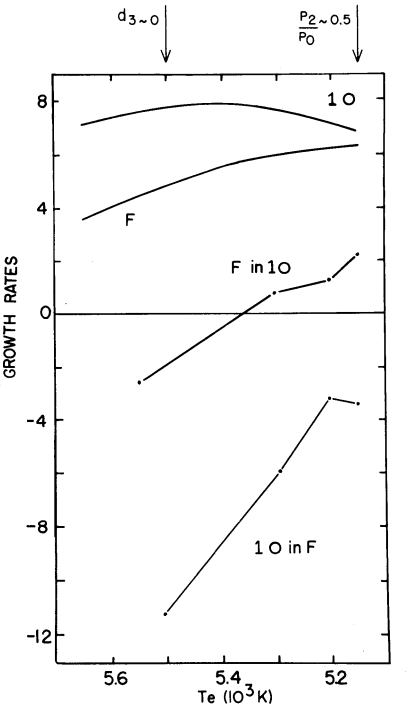

FIG. 4.—F and 1O growth rates versus effective temperature. The two upper curves give LNA growth rates according to S80. They have been shifted to the right by 150 K (see text). Lower curves give stability of F and 1O limit cycles as determined by periodic integrations with DYNSTAR.

DYNSTAR and represent the growth rates of F in 1O, and 1O in F, respectively. The two upper curves give linear growth rates calculated with the finely-zoned models of S80. The latter curves have been shifted to the right by 150 K in order to match up DYNSTAR and S80 period ratios as well as possible (see § II). The approximate locations of the two resonance centers are indicated at the top of the diagram.

The most interesting of the curves in Figure 4 is the one representing the growth of first overtone perturbations about the fundamental limit cycle (1O in F). While these perturbations suffer extremely strong damping in the model at 5500 K, by the time the 5200 K model is reached this damping has weakened considerably. The rise of the 1O in F curve is qualitatively in agreement with the results of Stellingwerf (1975*a*, *b*). In fact, had the maximum of this curve crossed the zero line, a narrow region of double-mode pulsation would have been indicated according to Stellingwerfs categories. On the other hand, we note that our 1O in F curve turns down slightly after reaching a peak, in contrast to the Stellingwerf calculations where the curve continues to rise. This downturn could be consistent with the results reported by Cox, Hodson, and Davey (1976).

The powerful damping encountered at 5500 K may be attributed to the fact that this model represents the estimated center of the interaction resonance $\omega_1 + \omega_0 = \omega_3$ for the DYNSTAR series. (The calculated center occurs at $\sim$5650 K for the models of S80.) Figure 5 shows the interior run of the second-order interaction amplitude μ_{r+} in the 5650 K model of S80. The trinodal resonant structure is evident (see S80). We note that the interaction amplitude is extremely strong, not only in the H I ionization zone, but also near the He II ionization zone, and even further inward (compare, e.g., the runs of μ_{r+} given in Figs. 5 and 6 of S80). If, in the simple interpretation of the previous section, the interaction terms always provide damping, then it is not surprising that this damping should be most effective when the interaction is strongest.

As one moves coolward of the resonance center, the interaction begins to weaken. However, a competing effect may be noted from Figure 4—namely, that the linear driving in 1O also begins to decline. In our interpretation, it is the former of these effects that produces the rise of the 1O in F curve, and the latter that gives rise to the subsequent downturn.

For the fundamental, the situation is somewhat different. At 5500 K, where the interaction is strongest, the fundamental is still suppressed (F in 1O < 0), but by the time one reaches the 5300 K model, the

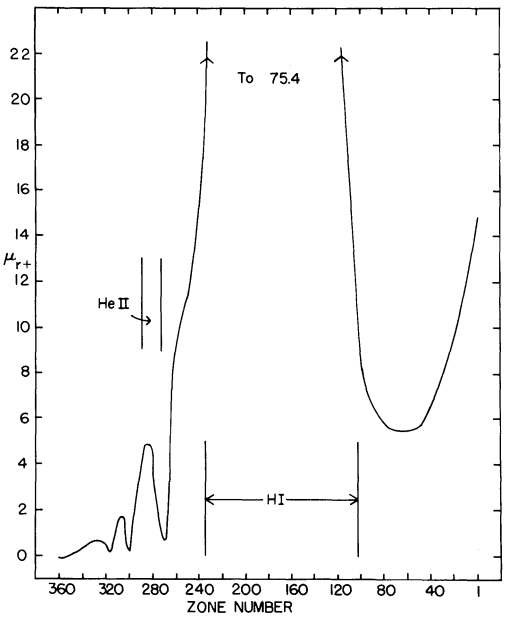

FIG. 5.—Second-order interaction amplitude μ_{r+} versus zone number for the 5650 K model of S80. H I and He II ionization zones are indicated.

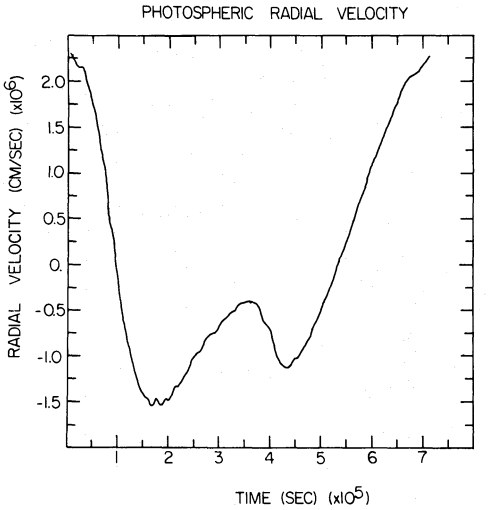

FIG. 6*a*

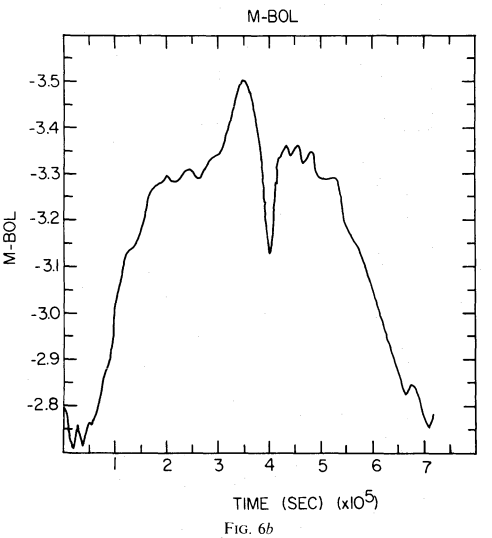

FIG. 6*b*

FIG. 6.—Fundamental limit cycle oscillations at photosphere of 5150 K DYNSTAR model. (*a*) Radial velocity ("observational" coordinates); (*b*) M_{BOL}.

transition line has already been crossed and F is able to grow in 1O. In contrast to the downturn noted in the 1O in F curve, the F in 1O curve continues to rise. Presumably, this is due to the fact that the linear driving in F has not yet saturated (see Fig. 4). In addition, the iterative interpretation suggests that, in general, interactive damping ought to suppress 1O more effectively than it suppresses F. The reason for this is that the third-order interactive corrections to F (see § III) arise from the interaction of certain second-order terms with the linear eigenfunction of 1O, while the corrections to 1O involve the interaction of the same second-order terms with the linear eigenfunction of F. Since the fundamental linear eigenfunction is everywhere larger than that of the overtone, it follows that the interactive damping of 1O ought to be favored.

As a final illustration of connections which appear between the resonance-influenced iterative amplitudes of S80 and the present hydrodynamic calculations, we wish to consider the DYNSTAR model at 5150 K ($\sim$5300 K in S80). The period ratio for the S80 version of this model is $P_2/P_0 = 0.498$ which puts it very near the center of the harmonic resonance. Figures 6*a* and 6*b* show the fundamental limit cycle at the photosphere of this model in radial velocity and $M_{\rm BOL}$, respectively. (The former plot is made in "observational" coordinates.) One sees from these curves a clear reinforcement of the idea that Cepheid "bumps" are connected with the resonance $P_2/P_0 = 0.5$, the double maximum structure appearing, as predicted, near the resonance center (Simon and Schmidt 1976; Simon 1977).

In addition, it is interesting to note that the limiting amplitudes for the 5150 K model displayed in Figure 6 are noticeably smaller than those attained by slightly hotter models. (For example, in the DYNSTAR model at 5300 K, the peak-to-peak velocity velocity amplitude is about 52 km s^{-1}, while $\Delta M_{\rm BOL} \sim 1.0$.) This dip in amplitude is actually observed at a period of approximately 10 days in the classical Cepheids (Ledoux and Walraven 1958; van Genderen 1974). In the iterative interpretation, it may be explained as the result of enhanced harmonic (i.e., single-mode) damping occasioned by the great strength of the second-order harmonic correction (β_r, in the notation of S80; see Fig. 7 of that paper) in models near the resonance center.

Finally, we remark that the redward rise of the 1O in F curve (Fig. 4) gives some hope that models not too different from the present ones may yet be successful in satisfying the Stellingwerf criterion of instability of both limit cycles. One possible alteration which comes to mind involves the artificial viscosity, whose effects on modal selection still require detailed examination. The results of the present investigation, while, strictly speaking, negative with respect to the resonance hypothesis, have tentatively established a relationship between resonances and modal selection and produced models which tend toward double-mode pulsation in the region between $\omega_1 + \omega_0 = \omega_3$ and $P_2/P_0 = 0.5$. The above results suggest that this domain of resonant interaction ought to be explored further.

One of us (N.R.S.) is pleased to acknowledge funding for this investigation by the National Science Foundation under grant AST 77-10155. We are also grateful to R. F. Stellingwerf for interesting and informative discussions.

REFERENCES

Baker, N. H., and von Sengbusch, K. 1969, *Mitt. Astr. Gesellschaft*, No. 27, p. 162.
Christy, R. F. 1966, *Ap. J.*, **144**, 108.
Cox, A. N. 1979, in *Proceedings of the Conference on Current Problems in Stellar Pulsation Instabilities*, in press.
Cox, A. N., Hodson, S. W., and Davey, W. R. 1976, in *Proceedings of the Solar and Stellar Pulsation Conference*, ed. A. N. Cox and R. G. Deupree (LASL: LA6544 c), p. 188.
Cox, A. N., Hodson, S. W., and King, D. S. 1978, *Ap. J.*, **220**, 996.
Faulkner, D. J. 1977, *Ap. J.*, **216**, 49.
Hodson, S. W., and Cox, A. N. 1976, in *Proceedings of the Solar and Stellar Pulsation Conference*, ed. A. N. Cox and R. G. Deupree (LASL: LA6544 c), p. 202.
Hodson, S. W., Stellingwerf, R. F., and Cox, A. N. 1979, *Ap. J.*, **229**, 642.
King, D. S., Cox, J. P., Eilers, D. D., and Davey, W. R. 1973, *Ap. J.*, **182**, 859.
Ledoux, P., and Walraven, Th. 1958, *Hdb. d. Phys.*, **51**, 353.
Niva, G. D. 1979, *Ap. J. (Letters)*, **232**, L43.
Shobbrook, R. R., and Faulkner, D. J. 1979, preprint.
Simon, N. R. 1972, *Astr. Ap.*, **21**, 45.
———. 1977, *Ap. J.*, **217**, 160.
———. 1979*a*, *Astr. Ap.*, **75**, 140.
———. 1979*b*, *Astr. Ap.*, **74**, 30.
———. 1980, *Ap. J.*, **237**, 175 (S80).
Simon, N. R., and Sastri, V. K. 1972, *Astr. Ap.*, **21**, 39.
Simon, N. R., and Schmidt, E. G. 1976, *Ap. J.*, **205**, 162.
Stellingwerf, R. F. 1974, *Ap. J.*, **192**, 139.
———. 1975*a*, *Ap. J.*, **195**, 441.
———. 1975*b*, *Ap. J.*, **199**, 705.
Stobie, R. S. 1969, *M.N.R.A.S.*, **144**, 485.
van Genderen, A. M. 1974, *Astr. Ap.*, **34**, 279.

ARTHUR N. COX and STEPHEN W. HODSON: Theoretical Division, Los Alamos Scientific Laboratory, P.O. Box 1663, Los Alamos, NM 87545

NORMAN R. SIMON: Behlen Laboratory of Physics, University of Nebraska, Lincoln, NE 68588